Interaction of amiloride and one of its derivatives with Vpu from HIV-1: a molecular dynamics simulation

V. Lemaitre[a,b], R. Ali[a], C.G. Kim[a], A. Watts[a], W.B. Fischer[a,c,*]

[a] *Biomembrane Structure Unit, Department of Biochemistry, Oxford University, South Parks Road, Oxford OX1 3QU, UK*
[b] *Nestec S.A., BioAnalytical Science Department, Vers-Chez-Les-Blanc, CH-1000 Lausanne 26, Switzerland*
[c] *Bionanotechnology Interdisciplinary Research Consortium, Clarendon Laboratory, Department of Physics, Oxford University, Parks Road, Oxford OX1 3SU, UK*

Received 26 January 2004; revised 26 February 2004; accepted 2 March 2004

First published online 15 March 2004

Edited by Maurice Montal

Abstract Vpu is an 81-residue membrane protein, with a single transmembrane segment that is encoded by HIV-1 and is involved in the enhancement of virion release via formation of an ion channel. Cyclohexamethylene amiloride (Hma) has been shown to inhibit ion channel activity. In the present 12-ns simulation study a putative binding site of Hma blockers in a pentameric model bundle built of parallel aligned helices of the first 32 residues of Vpu was found near Ser-23. Hma orientates along the channel axis with its alkyl ring pointing inside the pore, which leads to a blockage of the pore.

Key words: Viral ion channel; Vpu; HIV-1; Molecular dynamics simulation; Drug–protein interaction

1. Introduction

Vpu is an 81-amino acid protein encoded by HIV-1 with a high degree of sequence conservation [1]. Its function in the life cycle of HIV-1 is twofold: (i) to interact with CD4 in the endoplasmic reticulum to initiate the ubiquinine-mediated degradation of the CD4–Vpu complex and (ii) to enhance particle release at the site of the plasma membrane altering the electrochemical gradient via ion channel formation by homo-oligomerisation [2] in the lipid membrane. Whilst the first function is fairly established, the second is still open to debate [3]. It is still not unambiguously established whether ion channel activity is an intrinsic property of Vpu. If so, then a selective blocker needs to be found to give proof, which has been reported using the derivatives of amiloride (Am) [4]. There are reasonably good structural data available to permit generation of molecular models of Vpu (for an overview see [5,6]), in which there is a helical transmembrane (TM) domain followed by a larger cytoplasmic domain with a helix-loop helix-helix/turn motif. Such models can be used in molecular dynamics simulations to investigate the mechanism of function and also to initiate computational blocker (leading possibly to drug) screening and development.

This study is based on recent findings that cyclohexamethylene amiloride (Hma), but not Am itself, blocks channel activity of both a peptide corresponding to the TM segment of Vpu and full-length Vpu when reconstituted into lipid bilayers [4]. A homo-pentameric bundle based on the first 32 amino acids of Vpu in a helical motif was generated. Simulations in the presence of the blocker aim to shed light on: (i) the site of action for the blocker with the protein, (ii) whether the blocker affects the integrity of the bundle, and (iii) the most favourable conformation adopted by the blocker. Calculations were performed with Am as the non-potent blocker for comparison. Two different protonation states for each blocker were simulated.

2. Materials and methods

2.1. Model building

A pentameric Vpu TM bundle based on the first 32 amino acids of Vpu (HV1H2), QPIPIVAIVA[10]LVVAIIIAIV[20]VWSIVIIEYR[30]KI, was generated with the program X-Plor 3.1 [7] based upon a protocol described in detail elsewhere [8,9]. This protocol generates symmetrical arrangements of five α-helices and was based on a simulated annealing procedure with short molecular dynamics (MD) simulations. The initial inter-helical distance was set to 0.94 nm. During a first stage, which involves the simulated annealing, five structures were generated based on van der Waals interactions. In the next stage (stage 2) each of these five structures was used as a starting point for the consecutive steps which take electrostatic interactions into account. At the end 25 structures were obtained. Inter-helical root mean square deviation (RMSD) values were calculated for each bundle and the bundle with the lowest average RMSD (i.e. the most symmetrical) was selected.

The structures of Am (3,5-diamino-6-chloro-*N*-(diaminomethylene)-pyrazinecarboxamide) and Hma (5-(*N*,*N*-hexamethylene) amiloride) in both a deprotonated (AM, HMA) and a protonated state (proton at the guanidinium group, AM^+, HMA^+) were generated by applying DS Viewer Pro 5.0 (Accelerys) and were consequently used in the AutoDock software [10] to locate the putative binding site of the blockers with Vpu. In total 10 runs were performed with 30 000 energy minimisation steps. The conformation of the bundle was kept rigid, whilst the blocker was allowed to be flexible. All structures located the energetically most favourable site within the pore close to the serine residues. From a total of 200 putative docking conformations, the one closest to one of the serines was chosen for MD simulations. The respective blockers were then placed inside the pore. The system was then subjected to a 300-ps equilibration keeping only the position restraints on the backbone of the protein. The topology of each of the blockers was determined by manually adapting the output of PRODRG [11] for the force field GROMOS43a2.

2.2. MD simulations

The in-silico bundle was placed in a lipid bilayer consisting of 96 lipid molecules (1-palmitoyl-2-oleoyl-*sn*-glycerol-3-phosphatidylcholine, POPC) in which a hole, already generated by removing enough lipids to avoid any overlap with the bundle, was present [12]. The

*Corresponding author. Fax: (44)-1865-275234.
E-mail address: wolfgang.fischer@bioch.ox.ac.uk (W.B. Fischer).

0014-5793/04/$30.00 © 2004 Published by Elsevier B.V. on behalf of the Federation of European Biochemical Societies.
doi:10.1016/S0014-5793(04)00251-0

bilayer–bundle system was consequently solvated with 40 water molecules per lipid to give a system of around 20 000 atoms per experiment. As each helix has a net charge of +1, five chloride ions (six in the presence of the protonated blocker) were also added to compensate for any extra charge within the simulation box. The solvated system was equilibrated for 300 ps with the peptide restrained, followed by the production phase of fully unrestrained 12-ns MD simulation.

For MD simulations GROMACS v3.1.4 software was used. Simulations were run at 300 K in an isothermal–isobaric ensemble (NPT). Periodic boundaries were present and a Berendsen temperature and pressure coupling was chosen to keep these parameters constant. The time step for the simulation was 2 fs. A LINCS algorithm was used to maintain the geometry of the molecules. Long-range electrostatics were calculated with the particle-mesh Ewald (PME) method using standard GROMACS parameters: grid dimensions 0.12 nm, interpolation order 4. Double counting correction for short-range forces was applied. Lennard–Jones and short-range Coulomb interactions were cut off at 1.1 and 0.9 nm, respectively. The simple point charge water model [13] was used to describe the water in the simulation box. Simulations were performed on a Dell Precision 420 with a dual Pentium III 1 GHz processor or on a Dell Precision 330 with a Pentium IV 1.5 GHz. The pore radii were calculated using HOLE2 [14] with radii not being considered if larger than 1.0 nm.

3. Results

The site of Am–Vpu interaction and that of its derivative Hma with Vpu was elucidated by a docking approach. Independent of the number of TM helices the most likely binding site proposed for both blockers is around Ser-23 (Fig. 1, top pictures). At the starting structure, the guanidinium group of each of the blockers points towards the serine residues of the bundle. At the end of the simulations the blockers remain at the site of Ser-23. A view down the pore from the C- to the N-terminus reveals that both Am (Fig. 1A) and Hma (Fig. 1B) stay in contact with two helices most of the time (Fig. 1, bottom pictures). Independent of the protonation state, Am seems to allow more space within the pore for water or ions to pass through than Hma.

3.1. The protein

The RMSD of the backbone atoms for each of the simulated pentamers, without blocker and in the presence of either AM^+ (Fig. 2A) or HMA^+ (Fig. 2B), remains below 0.35 nm with respect to their initial conformations. The presence of AM and AM^+ does not have any impact on the RMSD. In both cases the curve can hardly be distinguished from the bundle without blocker. In the presence of HMA the bundles show some deviation from the bundle without blocker. Over a time span of the first 6 ns the RMSD values for the bundle with either of the blockers are slightly higher than the bundle without blocker. After another 6 ns the bundle with the HMA^+ remains approximately 0.05 nm higher than the value for the bundle without blocker. The RMSD for the bundle with the HMA approaches the value of the plain bundle.

The averaged root mean square fluctuation (RMSF) per residue (data not shown) of the bundle is indicative of a larger deviation of more than 0.3 nm for residues on the C-terminal end than on the N-terminal end. This is in common for all the simulations independent of the presence of the blocker and its protonation state and indicative of a loss of helicity (DSSP analysis, data not shown) [15]. For the membrane-spanning amino acids, the fluctuation is below 0.15 nm.

The presence of either of the blockers in the deprotonated state does not have a major impact on the overall structure of

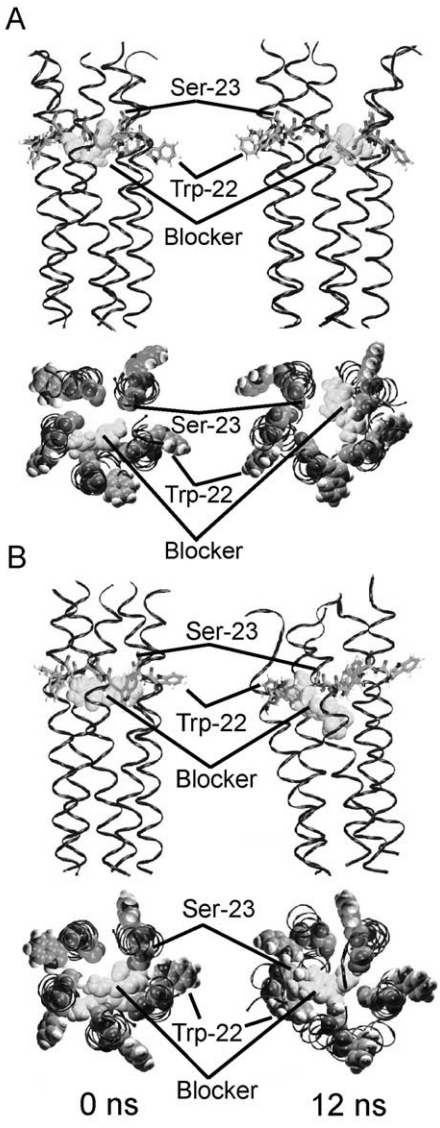

Fig. 1. Representation of the pentameric bundle of the TM part of Vpu in the presence of AM^+ (light grey, van der Waals representation) in a side view (upper panel) and view from the C-terminus into the pore (lower panel) (A). The peptide bundles are shown as ribbons (black). Tryptophans and serines are highlighted as sticks (grey scale is used). Lipid and water molecules are omitted for clarity. HMA^+ (light grey) is shown in the same way (B).

the bundle. The averaged tilt angle for the bundle without blocker is about $5.8 \pm 2.7°$, whilst the values for the bundles in the presence of the deprotonated blockers do not exceed $11.0 \pm 4.1°$. AM^+ and HMA^+ induce larger averaged tilt angles of $19.6 \pm 3.5°$ and $14.9 \pm 7.5°$, respectively. Changes for the average kink angle and cross angle are small but significant (with a confidence interval of 99.99%) indicating that the blockers do affect the properties of the bundle. The average inter-helical distances of the helices do not change in the presence of any of the blockers.

The pore is divided into three areas to refine the analysis of the effect of the blockers on the pore, the N-terminal (residues 1–11), middle (residues 12–22) and the C-terminal sections (residues 23–32). Time averages for the averaged minimum radii have been computed for each of the sections and are displayed in Table 1. Simulation of the bundle without any

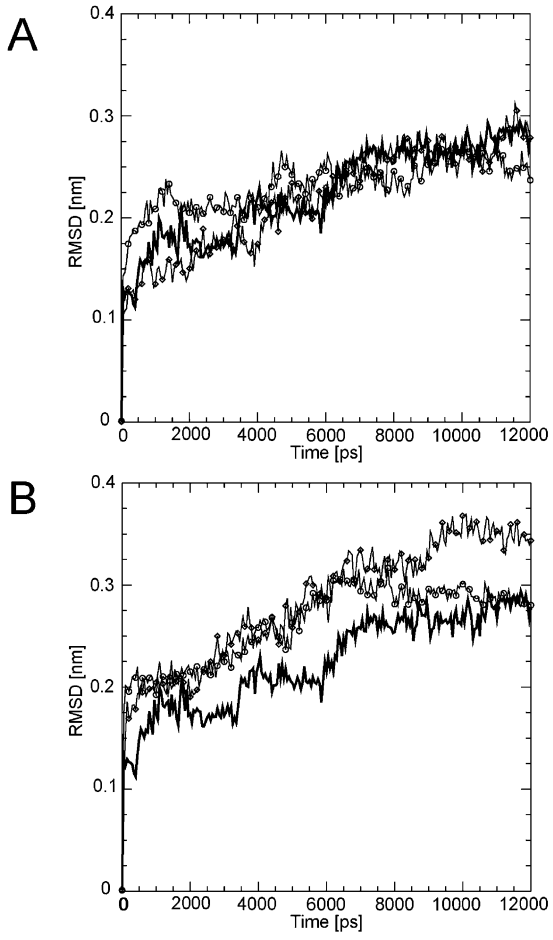

Fig. 2. RMSD of the Cα traces for the pentameric bundle without blocker (black line), and in the presence of protonated (diamonds) and deprotonated (circles) blockers. Am (A) and Hma (B).

blocker reveals a minimum pore radius of 0.12 ± 0.06 nm for the C-terminal section. The simulation with AM^+ shows an opening of the bundle, with an average radius of 0.21 ± 0.05 nm. The same calculation, taking into account the presence of the blocker and the consequent obstruction of the pore resulting from it, allows computation of the apparent pore radius and reveals a slightly smaller radius of 0.20 ± 0.06 nm. HMA^+ also induces a larger pore radius at this section of the bundle with values of 0.19 ± 0.06 nm (and for the apparent pore radii: 0.18 ± 0.06 nm). The middle section remains almost unaffected by the blockers. Average radii of 0.18 ± 0.02 nm (AM^+) and 0.17 ± 0.03 nm (HMA^+) are close to the value for the bundle without any blocker at 0.18 ± 0.03 nm. However, the presence of the blockers decreases the calculation of the apparent radii to 0.14 ± 0.05 nm (for AM^+) and 0.06 ± 0.04 nm (for HMA^+). The pore radius in the presence of HMA^+ would not even allow for a single-file water passage as found in gramicidin A [16,17]. Thus, HMA^+ completely blocks the pore. At the N-terminal section, an average pore radius of 0.11 ± 0.04 nm is calculated without the presence of the blocker in the pore. The presence of AM^+ is accompanied by a widening of up to 0.17 ± 0.04 nm for the N-terminal section. In the presence of HMA^+ the pore narrows (0.13 ± 0.05 nm) compared to the simulations with an empty bundle.

Simulations with the blockers in a neutral state were also performed. Although this state is unlikely to happen in nature, it allows us to gain more insight into the blocker–protein interactions by performing 'impossible' virtual experiments. Removing the electrical charge on the guanidinium group (deprotonated blockers) leads to an overall narrowing of the pore radii in all three sections (Table 1). The decrease of the pore opening is more pronounced for the simulations with AM, particularly in the middle section with a radius of 0.14 ± 0.03 nm. For HMA, there is a widening of the pore radius in the middle section (0.06 ± 0.04 nm C-terminal section, 0.16 ± 0.04 nm middle section, 0.09 ± 0.04 nm N-terminal section). In the middle section the apparent radii decrease to 0.08 ± 0.03 nm and 0.07 ± 0.03 nm for AM and HMA, respectively. The two deprotonated blockers result in a blocking of the C-terminal part with almost identical apparent radii of ~0.05 nm.

To summarise the results, AM^+ and to a lesser extent HMA^+ lead to a widening of both the C- and N-terminal sections. In the presence of HMA^+, the diameter of the N-terminal section is reduced compared to the simulations of the Vpu bundle in the presence of AM^+. HMA^+ induces a 'funnel'-like shape in the pore, in addition to an almost complete obstruction of the middle section of the pore. Simulating the unrealistic situation, where charges on the blockers are removed, leads to an overall narrowing of the pore. The blocking resulting from the presence of HMA seems to occur mainly by occlusion of the pore. These changes, although relatively small, are found to be significant at a confidence level of 99.99%.

Water molecules are found only within the pore at the C-terminal end approaching the blockers during the entire length of the simulations. Towards the N-terminal end, for which the pore is lined by highly hydrophobic residues, no water molecules can be detected. The water molecules, which are present when each of the models is built, escape from the pore during the 300-ps equilibration step and do not re-enter the pore during the simulation.

3.2. The blocker

The RMSD values for AM and AM^+ (data not shown) do not exceed 0.15 nm within the duration of the simulation. The RMSD values for HMA and HMA^+ remain around 0.15 nm, with a larger fluctuation for the latter (0.1 nm < RMSD < 0.2 nm). The larger values and spread are due to the flexible hexamethylene ring of the AM derivative. These values are

Table 1
Averaged minimum pore radii of the pentameric bundle when divided into three sections: the C-terminal (C), middle (M) and N-terminal (N) sections

	C (nm)	M (nm)	N (nm)
Vpu	0.12 ± 0.06	0.18 ± 0.03	0.11 ± 0.04
Bundle (+AM^+)	0.21 ± 0.05	0.18 ± 0.02	0.17 ± 0.04
Bundle+AM^+	0.20 ± 0.06	0.14 ± 0.05	0.17 ± 0.04
Bundle (+HMA^+)	0.19 ± 0.06	0.17 ± 0.03	0.13 ± 0.05
Bundle+HMA^+	0.18 ± 0.06	0.06 ± 0.04	0.13 ± 0.06
Bundle (+AM)	0.05 ± 0.03	0.14 ± 0.03	0.09 ± 0.03
Bundle+AM	0.05 ± 0.03	0.08 ± 0.03	0.09 ± 0.03
Bundle (+HMA)	0.06 ± 0.04	0.16 ± 0.04	0.09 ± 0.04
Bundle+HMA	0.05 ± 0.04	0.07 ± 0.03	0.08 ± 0.04

Each segment is of equal length (approximately 12 amino acids). Minimum pore radii were averaged over the entire length of each simulation. The apparent radii are calculated with (e.g. bundle+HMA^+) and without (e.g. bundle (+HMA^+)) considering the blockers in the pore.

within the range of values obtained for K^+ channel blocker toxins simulated in aqueous solution [18]. In addition, the RMSFs of the individual atoms of the blockers support this result. The central bodies of Am (a 3,4,6-substituted pyrazine ring) and Hma remain fairly rigid (RMSF < 0.1 nm) independent of the protonation state of the blockers. Only the hydrogen atoms of the amino groups of the pyrazine ring show an RMSF slightly above 0.1 nm. For both blockers the hydrogen atoms of the guanidinium group show the largest RMSF (> 0.1 nm). Overall, the curves are very similar for both blockers when compared to similar atoms with lower values for all atoms in the protonated blocker. The atoms of the hexamethylene ring in Hma are seen to fluctuate around 0.1 nm. The protonation state does not affect the fluctuation of this part of the molecule.

The different conformations generated during the MDs for all four blockers tested were clustered using a full linkage algorithm, with a cut-off of 0.03 nm for Am and 0.04 nm for Hma. In the case of AM, this means that molecules with an RMSD smaller than 0.03 nm relative to all the existing members of a cluster will belong to this cluster. Cluster analysis reveals the most populated conformation for each of the blockers (Fig. 3). AM^+ (Fig. 3A) and AM (Fig. 3B) spend 96.0% and 87.9%, respectively, of their time in this conformation. For HMA^+ (Fig. 3C) and HMA (Fig. 3D) the values are 95.1% and 91.5%, respectively. For the protonated blockers, the carbonyl group linked to the guanidinium group points towards the primary amine group of the pyrazine ring. Deprotonation of the blockers reveals a conformational change in the blocker so that the amine part of the guanidinium group now points to the primary amine group of the pyrazine ring.

The AM^+ forms on average 1.3 hydrogen bonds with water molecules during the simulation. The threshold for hydrogen bonding was A–H < 2.5 Å and an angle A–H–D < 60°, with A defining the acceptor, D the donor. The number of hydrogen bonds indicates that, on average, more than one hydrogen bond is formed between the blocker and the solvent. About 0.82 hydrogen bonds are formed with the side chains of the serine residues and about 0.19 hydrogen bonds with the backbone of the peptide. Barely any hydrogen bonds are formed with the tryptophan side chains. For AM, the total number of hydrogen bonds is reduced in the following order: serine side chain (0.42), solvent (0.14), almost no interactions with the backbone (0.08) and tryptophans (0.00). For HMA^+, the water molecules are also the most frequent hydrogen bond contacts with the blocker (1.7), followed by hydrogen bonding to the serine side chains (0.77) and tryptophan (0.26). Tryptophans are no longer significantly involved in hydrogen bonding with HMA (0.02). As a result, AM^+ interacts mainly with the serine side chains, whilst HMA^+ also interacts with the tryptophans.

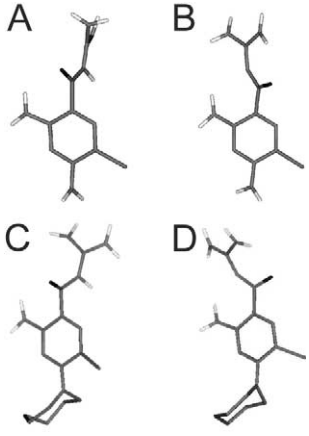

Fig. 3. Most frequently occupied conformations of Am (A: protonated, B: deprotonated) and Hma (C: protonated, D: deprotonated).

Am remains with its long axis almost parallel to the membrane plane independent of its protonation state: 5.3 ± 23.3° protonated, 8.6 ± 51.8° deprotonated. The large standard deviation is due to the frequent reorientation of the blocker. Rotational motion around the membrane normal (*z*-axis), in the plane of the membrane (*x*-*y* plane), is indicated by oscillations in the range of ± 40° for AM^+. Hma, however, is more likely to orientate itself out of the membrane plane towards the membrane normal: 43.0 ± 11.8° protonated, 11.3 ± 12.7° deprotonated. The hexamethylene ring also orientates itself towards the hydrophobic N-terminal end of the bundle. The lower standard deviation is indicative of a relatively narrow band of possible orientations held for a relatively long time during the simulations. HMA^+ screens for the hydrophobic area of the pore with its hydrophobic methylene ring. Rotation around the membrane normal is restricted to slight fluctuations around −15° for HMA^+.

4. Discussion

In a recent publication [4] the blocking of both full-length Vpu and a peptide corresponding to the TM segment of Vpu reconstituted into lipid membranes by Am derivatives has been demonstrated. Also the viral ion channel p7 from hepatitis C virus can be blocked by the Am derivative, Hma [19]. With the present investigations we aim to shed light on the mechanism of interaction between these blockers and a Vpu bundle. The computational model of the bundle is based on the available structural and functional information in the literature (for an overview see [5,6]).

4.1. Plausibility of the bundle model

There is computational and experimental evidence which supports a model where Vpu adopts a pentameric oligomerisation state. Early computational studies based on the TM part of Vpu were performed with constrained pentameric and hexameric bundles [20]. The potential energy profiles of the interactions of a cation and an anion with the pore are in favour of the cation for the pentameric bundle, which supports the idea of a pentameric oligomerisation state of the bundle. In an experimentally driven approach using Fourier transform infrared (FTIR) spectroscopy, a pentameric bundle showed the lowest potential energy profile and matched most closely the experimentally derived data, such as the tilt angle of the peptide inserted into lipid membranes [21]. Comparison of conductance data with model calculations excludes a tetrameric assembly and supports the pentameric model [15]. Furthermore, recent MD simulations show instabilities of hexameric bundles of Vpu compared to pentameric bundles, which is interpreted as another indication of the pentameric model as the working model [22].

The consideration of how to build bundles of Vpu has been discussed previously in detail elsewhere [9]. In brief, the ser-

ines point into the pore which moves the tryptophans to the outside of the bundle. The orientation of hydrophilic residues, such as serines, towards the pore is also established for the nicotinic acetylcholine receptor [23,24]. The consequent position of the tryptophans in the bundle model of Vpu has its experimental verification in the fact that helical membrane proteins, such as bacteriorhodopsin [25,26], as well as β-barrel pores, such as porins [27], have these amino acids anchoring the protein within the membrane. The macroscopic analysis of the computational bundles, such as the average tilt angles of the bundle, falls within the range found experimentally (for an overview see [6]). The average tilt angle for the bundle without blocker ($5.8 \pm 2.7°$) seems to be lower than the most recent experimentally derived value of 13° from nuclear magnetic resonance spectroscopy [28] and closer to the value derived from FTIR spectroscopy ($6.5 \pm 1.6°$) [21]. The differences may arise from the use of TM segments which differ in length. The different lipids used in the individual approaches and the consequent phase conditions they impose may also account for the differences. The kink angle calculated from the present bundle structure, taking the Cα atoms of the residues Ile-16 to Ala-18 as centre points, is slightly lower compared to the experimentally derived values [28]. However, calculations of the kink angle for the extended model Vpu_{1-52} as a single entity in the lipid bilayer [29] fit well with the experimentally derived data [28]. In the current model, the arginine residues point into the pore in such a way as to compensate the selectivity for cations. However, the arginine side chain is very flexible and is able to occupy a large conformational space by swinging in and out of the pore. In a kinked model, the arginine shows large movements during the simulations [29]. This flexibility might have an impact on the electrostatic profile of the C-terminal mouth of the channel and its ion selectivity. As a consequence anions could pass without being trapped by the positive charges. Glutamate and lysine, the other charged residues present at the C-terminal end, are positioned at the outside of the bundle and are proposed to be involved in clamping of the bundle [6]. The clamp might be weak and permit a dynamic behaviour of the bundle on a biologically relevant time scale. These dynamics could also allow the flux of larger ions, such as phosphate ions, through the pore [30].

Consequently, the present model is a reasonably good model for the simulations on a Vpu bundle.

The missing water molecules within the pore towards the N-terminal end reflect the strong hydrophobic character of this part of the TM segment combined with the small pore radius. Earlier calculations using cut-off radii for the treatment of electrostatic interactions revealed continuous water columns within the pentameric bundle [15]. Recent investigations of theoretical hydrophobic pore models using PME calculations show that the presence of water in these pores is strongly dependent on the pore radius and on membrane polarisation effects [31–33]. In addition the Lennard–Jones parameters of the water molecules [34] and the hydrophobic/hydrophilic character of the walls with which the waters can interact affect the presence of water molecules [35]. Regarding the pore radius, below a certain threshold diameter water molecules would not pass through a pore [31,33]. With increasing pore size, water will eventually pass in an intermittent way [31,32] or 'avalanche-like fashion' [33]. Simulations on longer time scales are needed to assess the proper behaviour of the water molecules in confined geometries. A protein model from the mechanosensitive channel MscS, with a narrow hydrophobic part (hydrophobic lock) within the pore similar to Vpu, also shows the escape or 'dewetting' of this part of the pore [36]. The Vpu bundle model used might represent a proper bundle with a temporary state of low water content. It is possible that the hydrophobic part contributes to the low conductance found for the peptide corresponding to the TM segment of Vpu and reconstituted into lipid membranes [28,30].

4.2. Plausibility of the blocker–protein binding site

Am is a molecule with a considerable number of hydrogen bond donor groups (amino functions) capable of forming hydrogen bonds with hydrogen bond acceptors, such as the serines. Consequently the C-terminal end of the Vpu bundle with the serines as putative hydrogen bond acceptors should be a plausible binding site. In addition, the tryptophans, in an equilibrated bundle model located at the helix/lipid interface, may also act as hydrogen bond acceptors. Glu-28, which is located at the outside of the bundle and could be a hydrogen bond acceptor, has been found not to interact with either blocker in a pure docking approach (C. Kim, V. Lemaitre, A. Watts and W.B. Fischer, to be published). The positive charge of Arg-30 points into the pore (at pH 7) and seems to have only the chloride atom and the carbonyl oxygen atom of the blockers as putative electrostatic counterparts.

With respect to the Am body, the same conclusion applies for Hma. The hydrophobic ring adds an amphipathic character to the blocker. This hydrophobic part is involved in hydrophobic interactions with hydrophobic residues of the bundle within the pore towards the N-terminal end. It should be noted that molecules containing several methyl groups have been found to block voltage-gated sodium channels from frog nerve axons independent of the overall size of the blockers [37]. This suggests that molecules carrying methyl groups, or Hma with its hexamethylene ring share a common blocking mechanism.

4.3. Experimentally and computationally derived evidence for a binding site and binding geometry of amiloride and other blockers in ion channels

Hydrophobic interactions with parts of the channel adjacent to the AM binding site have been found to increase the binding affinity of the blocker [38]. For Am, a putative binding site in the Na^+ channel has been proposed to be approximately 20% within the transmembrane electrical field [39,40] on the extracellular side [41]. The orientation allows the guanidinium group to penetrate into the pore (reviewed in [42]). A point mutation within the TM region replacing a crucial serine residue also abolishes affinity for Am [43]. Consequently, the binding site proposed, with the guanidinium group in the vicinity of the serines of the putative pore of Vpu in the present study, is in agreement with findings on the epithelial sodium channel.

4.4. Effect of hydrogen bonding

The protonated blockers are the physiologically relevant forms in aqueous solution. The positive charge on the blockers was removed in this study to evaluate the role of charge in the blocking mechanism. The trend of the data for the deprotonated blockers parallels the data of the protonated blockers with respect to their effect on the protein. Comparison of the

blocker data shows differences in conformation, a larger fluctuation of the guanidinium group and less hydrogen bonding for the deprotonated blockers. Deprotonation of the blocker results in a loss of hydrogen bond formation with the side chains serines and tryptophan, the backbone and water.

HMA^+ forms hydrogen bonds with tryptophan, with the consequence that this residue is moved towards the blocker into the helix–helix interface and almost into the pore (Fig. 1B). AM^+ and also AM form fewer hydrogen bonds on average suggesting a weaker interaction with the bundle. Hydrogen bonding and electrostatic interactions play a major role in the structural conformation of helical TM proteins/peptides in the vicinity of hydrophobic areas and also within them [44,45]. The low dielectric slab of a bilayer imposes a driving force to saturate any free hydrogen bond with a proton acceptor [46]. The locations of the guanidinium groups of the blockers and the serines are at the hydrophilic (headgroup region)/hydrophobic (hydrophobic slab of the bilayer) interface of the peptide bundle. Consequently the guanidinium group might anchor the blocker at this particular position.

4.5. Mode of action

The averaged radius of the pore depends on the presence of the blockers and in particular of HMA^+. A pronounced narrowing of the apparent aperture of the middle of the bundle is observed when HMA^+ is in the pore. For AM^+, the reduction in pore diameter is less and would therefore allow waters, and possibly ions with them, to pass the pore along an electrochemical gradient. The proposed mechanism of HMA^+ blocking might also involve interaction with the tryptophans. The increase in the tilt angle of the bundles in the presence of AM^+ and HMA^+ can be best explained by considering the helices as sliding along each other. This mechanistic view is supported by the observed increase in the cross angle.

In this study the situation is presented when the blocker has already reached its binding site. In our current bundle model, arginine side chains point approximately into the pore. Being at the entrance of the pore, the side chains are flexible and free to change their orientation, whilst the backbone is embedded within a helical environment. On the in vivo time scale these side chains may fluctuate, allowing the blocker to reach its binding site. Like other titratable residues, if close to each other [47], all arginines might not be simultaneously protonated. Temporary deprotonation of one arginine would allow for an attraction of the guanidinium group towards the arginines and the mouth of the pore. This attraction would lead to the embedding of the blocker in the pore as outlined.

5. Conclusions

The hydrophilic residue Ser-23 is a favourable binding site of the blockers. The mode of blocking of HMA^+, once it is in the pore, is that of steric hindrance. This steric hindrance is supported by a combination of factors such as hydrogen bond formation with tryptophan and implementation of slightly altered pore geometry. AM^+, although favouring the site within the bundle, is still able to allow for space for water molecules and ions to pass through. Regarding the pore radius, its impact on the pore is effectively opposite that of the derivative.

Acknowledgements: W.B.F. thanks the E.P. Abraham Research Fund for financial support of this work. The Engineering and Physical Science Research Council (EPSRC), Medical Research Council (MRC), the Biological Science Research Council, the Bionanotechnology IRC and CJ Corporation (for financial support to C.G.K.) are all acknowledged for grant support to A.W. We thank CCLRC-RAL for computer facilities and service.

References

[1] Willbold, D., Hoffmann, S. and Rösch, P. (1997) Eur. J. Biochem. 245, 581–588.
[2] Maldarelli, F., Chen, M.Y., Willey, R.L. and Strebel, K. (1993) J. Virol. 67, 5056–5061.
[3] Lamb, R.A. and Pinto, L.H. (1997) Virology 229, 1–11.
[4] Ewart, G.D., Mills, K., Cox, G.B. and Gage, P.W. (2002) Eur. Biophys. J. 31, 26–35.
[5] Bour, S. and Strebel, K. (2003) Microbes Infect. 5, 1029–1039.
[6] Fischer, W.B. (2003) FEBS Lett. 552, 39–46.
[7] Brünger, A.T. (1992) X-PLOR Version 3.1. A system for X-ray crystallography and NMR, Yale University Press, New Haven, CT.
[8] Kerr, I.D., Sankararamakrishnan, R., Smart, O.S. and Sansom, M.S.P. (1994) Biophys. J. 67, 1501–1515.
[9] Cordes, F., Kukol, A., Forrest, L.R., Arkin, I.T., Sansom, M.S.P. and Fischer, W.B. (2001) Biochim. Biophys. Acta 1512, 291–298.
[10] Morris, G.M., Goodsell, D.S., Huey, R., Hart, W.E., Halliday, S., Belew, R. and Olson, A.J. (1998) J. Comp. Chem. 19, 1639–1662.
[11] van Aalten, D.M.F., Bywater, R., Findlay, J.B., Hendlich, M., Hooft, R.W. and Vriend, G. (1996) J. Comput. Aid. Mol. Des. 10, 255–262.
[12] Fischer, W.B., Forrest, L.R., Smith, G.R. and Sansom, M.S. (2000) Biopolymers 53, 529–538.
[13] Berendsen, H.J.C., Griegera, J.R. and Straatsma, T.P. (1987) J. Phys. Chem. 91, 6269–6271.
[14] Smart, O.S., Neduvelil, J.G., Wang, X., Wallace, B.A. and Sansom, M.S.P. (1996) J. Mol. Graph. 14, 354–360.
[15] Cordes, F.S., Tustian, A.D., Sansom, M.S., Watts, A. and Fischer, W.B. (2002) Biochemistry 41, 7359–7365.
[16] Roux, B. and Karplus, M. (1991) Biophys. J. 59, 961–981.
[17] de Groot, B.L., Tieleman, D.P., Pohl, P. and Grubmüller, H. (2002) Biophys. J. 82, 2934–2942.
[18] Grottesi, A. and Sansom, M.S.P. (2003) FEBS Lett. 535, 29–33.
[19] Premkumar, A., Wilson, L., Ewart, G.D. and Gage, P.W. (2004) FEBS Lett. 557, 99–103.
[20] Grice, A.L., Kerr, I.D. and Sansom, M.S.P. (1997) FEBS Lett. 405, 299–304.
[21] Kukol, A. and Arkin, I.T. (1999) Biophys. J. 77, 1594–1601.
[22] Lopez, C.F., Montal, M., Blasie, J.K., Klein, M.L. and Moore, P.B. (2002) Biophys. J. 83, 1259–1267.
[23] Leonard, R.J., Labarca, C.G., Charnet, P., Davidson, N. and Lester, H.A. (1988) Science 242, 1578–1581.
[24] Revah, F., Galzi, J.L., Giraudat, J., Haumont, P.Y., Lederer, F. and Changeux, J.P. (1990) Proc. Natl. Acad. Sci. USA 87, 4675–4679.
[25] Pebay-Peyroula, E., Rummerl, G., Rosenbusch, J.P. and Landau, E.M. (1997) Science 277, 1676–1681.
[26] Sass, H., Buldt, G., Gessenich, R., Hehn, D., Neff, D., Schlesinger, J., Berendzen, J. and Ormos, P. (2000) Nature 40, 649–653.
[27] Pautsch, A. and Schulz, G.E. (2000) J. Mol. Biol. 298, 273–282.
[28] Park, S.H., Mrse, A.A., Nevzorov, A.A., Mesleh, M.F., Oblatt-Montal, M., Montal, M. and Opella, S.J. (2003) J. Mol. Biol. 333, 409–424.
[29] Sramala, I., Lemaitre, V., Faraldo-Gomez, J.D., Vincent, S., Watts, A. and Fischer, W.B. (2003) Biophys. J. 84, 3276–3284.
[30] Ewart, G.D., Sutherland, T., Gage, P.W. and Cox, G.B. (1996) J. Virol. 70, 7108–7115.
[31] Allen, R., Melchionna, S. and Hansen, J.-P. (2002) Phys. Rev. Lett. 89, 175502.1–175502.4.
[32] Allen, R., Hansen, J.-P. and Melchionna, S. (2003) J. Chem. Phys. 119, 3905–3919.
[33] Beckstein, O. and Sansom, M.S.P. (2003) Proc. Natl. Acad. Sci. USA 100, 7063–7068.

[34] Hummer, G., Rasaiah, J.C. and Noworyta, J.P. (2001) Nature 414, 188–190.
[35] Spohr, E., Trokhymchuk, A. and Henderson, D. (1998) J. Electroanal. Chem. 450, 281–287.
[36] Anishkin, A. and Sukharev, S. (2004) Biophys. J. (in press).
[37] Hille, B. (1971) J. Gen. Physiol. 58, 599–619.
[38] Garty, H. and Palmer, L.G. (1997) Physiol. Rev. 77, 359–396.
[39] Fyfe, G.K. and Canessa, C.M. (1998) J. Gen. Physiol. 112, 423–432.
[40] Li, J.H., Cragoe Jr., E.J. and Lindemann, B. (1987) J. Membr. Biol. 95, 171–185.
[41] Benos, D.J. (1982) Am. J. Physiol. 242, C131–C145.
[42] Alvarez de la Rosa, D., Canessa, C.M., Fyfe, G.K. and Zhang, P. (2000) Annu. Rev. Physiol. 62, 573–594.
[43] Waldmann, R., Champigny, G. and Lazdunski, M. (1995) J. Biol. Chem. 270, 11735–11737.
[44] Landolt-Marticorena, C., Williams, K.A., Deber, C.M. and Reithmeier, A.F. (1993) J. Mol. Biol. 229, 602–608.
[45] Chin, C.N. and von Heijne, G. (2000) J. Mol. Biol. 303, 1–5.
[46] Lew, S., Ren, J. and London, E. (2000) Biochemistry 39, 9632–9640.
[47] Tieleman, D.P., Breed, J., Berendsen, H.J. and Sansom, M.S. (1998) Faraday Discuss., 209–223.